UNIVERSITAT DE BARCELONA

Treball de Fi de Grau

GRAU D'ENGINYERIA INFORMÀTICA

Facultat de Matemàtiques i Informàtica
Universitat de Barcelona

Parkinson's Disease Brain States and Functional Connectivity: A Machine Learning Analysis of Neuroimaging Data

---

Lluís Montabes García

Director: Ignasi Cos Aguilera
Realitzat a: Departament de Matemàtiques
i Informàtica

Barcelona, 13 de setembre de 2020

Abstract

The goal of this study is to identify and characterize brain states as a function of the motivation with which the task was performed (the presence of avatars and their skill at performing the task). To this end, we developed a series of machine learning algorithms capable of capturing differences between the EEG data recorded at each condition. We used metrics of local activity, such as electrode power, of similarity (correlation between electrodes), and of network functional connectivity (co-variance across electrodes) and use them to cluster brain states and to identify network connectivity patterns typical of each motivated state.

Studies in the field of computational neuroscience involve the analysis of brain dynamics across specific brain areas to study the mechanisms underlying brain activity. This particular study aims at discovering how brain activity is affected by social motivation by computational means. To this end, we analyzed a dataset of electro-encephalographic (EEG) data recorded previously during a reward-driven decision-making experiment performed by Parkinson patients. The goal of the experiment was to select and perform a reaching movement from an origin cue to one of two possible wide rectangular targets. Reward was contingent upon arrival precision. Social motivation was manipulated by simulating avatar partners of varying skill with whom our participants played. Competition with the avatar was explicitly discouraged.

Our results show that the presence of different avatars yielded distinct brain states, characterized by means of functional connectivity and local activity. Specifically, we observed that motivation related states were best identified for the highest frequency band (gamma band) of the EEGs.

In summary, this study has shown that brain states can be characterized by level of motivation with a high degree of accuracy, independently of the presence of medication.

Acknowledgements

I want to thank, first and foremost, my supervisor Dr. Ignasi Cos for his incessant support, patience and helpfulness throughout the project. His support has been of paramount importance and there is no way this study could have been completed without him.

I must also thank fellow student of his, Michael A. DePass, for generously putting aside time to aid in the pre-processing of the data used in this study.

Lastly, I want to thank my friends and family for their invaluable assistance and encouragement.

Contents

1. Introduction

Systems' Neuroscience is the discipline devoted to the study of the physiology of the nervous system and their relationship with the principles that govern behavior[1]. Computational neuroscience is the sub-discipline that uses mathematical and analytical methods to this end – describing models of interaction capable of processing information and reproducing cognitive tasks.[2] This methodology has gained an unprecedented popularity during the last few decades thanks to the advances in computational power, increased popularity of non-invasive imaging technologies (such as fMRI or EEG) and remarkable progress of data analysis and machine learning techniques.

While brain activity remains mostly hidden from us, several technologies allow a partial observation and imaging of brain activity: 1) functional magnetic resonance imaging (fMRI), which measures changes associated with blood flow to identify functionally related brain areas, and 2) electroencephalography (EEG), which records electrical activity from the surface of the brain. Each one of these exhibits inherent advantages and drawbacks; while fMRI provides high spatial resolution, its temporal resolution is constrained to 1s, which lays far from the millisecond level physiological processes; furthermore, the cost of fMRI sessions is typically non-negligible. By contrast, EEG is inexpensive and offers millisecond level temporal resolution, which is counterbalanced by its limited spatial resolution.

The goal of this study is to identify patterns of brain activity related to specific motivated brain states in Parkinson's disease patients, and of the differential effect caused by their (dopaminergic) medication. Specific motivated states were induced during the performance of an experiment (see METHODS) in which patients had to perform in the presence of simulated partners ---avatars, which exhibited a lesser or better performance than theirs. Patients performed two sessions, ON/OFF medication, to be able to compare the effect of their medication on their behavior and brain states. To this end, we will use EEG segments extending hundreds of milliseconds around specific trial events. We used a Philips EGI recording system with 108 EEG electrodes. We developed a pipeline to clean the EEG data from artifacts and developed specific machine learning algorithms to categorize the brain states.

With this work, we intend to answer the following questions:

- Can motivational brain states be identified via machine learning methods from EEG recordings?

- Does the presence of medication affect brain activity in a similar manner to motivational state? Can we detect and quantify these effects with the same machine learning methods?

2. Methodology

2.1 Experiment Description

Our analyses are based on the recordings performed during performance of a reward-driven, decision-making task between two reaching movements, in which the participant must perform a precision arm reaching to attain reward. Participants were presented with a screen showing an origin cue (taking the form of a pale-blue dot with a radius of 1cm), a pointer which served as a virtual avatar for the participant (pale-blue dot with a radius of 1cm), and a delimited area into which the participant was instructed to move their virtual avatar (dark-blue square, 10cm side, 1cm depth). A motion tracker was attached to the arm of the participant, which allowed the virtual avatar to respond to its movements. The participant was rewarded for directing the avatar into the delimited target area with as much precision as possible. Maximum reward is attained by reaching the center of the target area, decreasing linearly with precision.

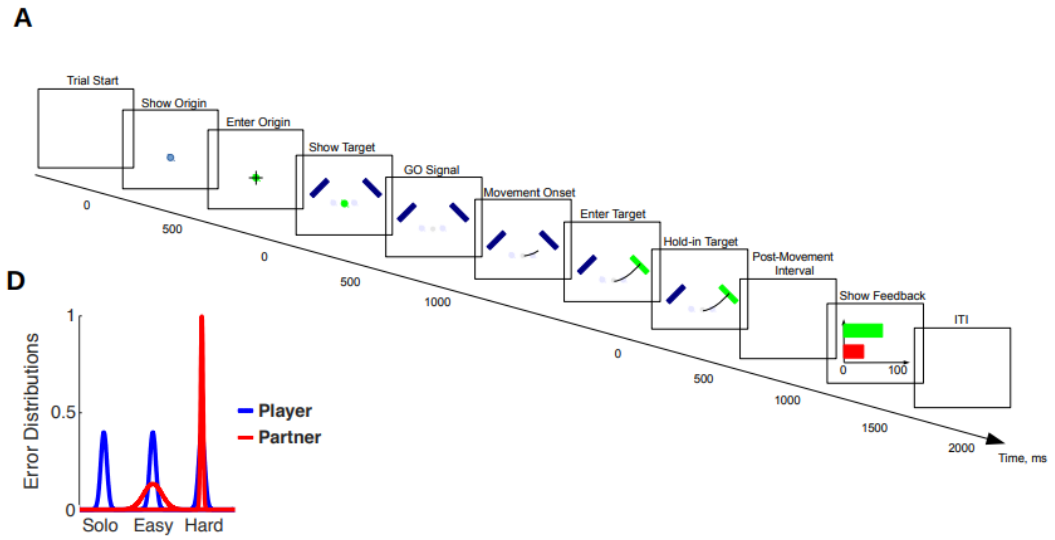

Figure 1. *Timeline of a trial and error distribution by simulated skill of the virtual partner.*

Three factors were varied throughout the experiment: motivation, biomechanics, and requirement of stopping at the target – in some cases, the participant was instructed to stop at the target ("Stop-In"); in others, to go through it and stop afterwards ("Punch-Through"). In order to induce higher states of motivation, a virtual opponent of increasing capabilities per desired level of motivation was introduced into the simulation. The participant was instructed to ignore the virtual opponent.

The experiment is divided into two equal sessions, which are themselves composed of six blocks containing 108 trials each – blocks 1-6 for session 1, blocks 7-12 for session 2. The conditions of the experiment vary by block: blocks 1, 3 and 5 are "Stop-In", while 2,

4 and 6 are “Punch-Through”. Blocks 1 and 2 had the participant playing without competition, blocks (3-4; 7-8) introduced a partner of low simulated skills and blocks (5-6; 9-10) introduced a skilled partner.

The trial started when the origin cue was displayed on the screen, and time began once the participant had placed their finger into the origin cue. 500ms later, two potential trajectories were shown on-screen, of which the participant had to choose one. A second later, the origin cue disappeared, signaling the participant to begin movement. Participants were instructed to make choices in the most unbiased possible manner, and to react as fast as possible.

100ms after entering the target area, the participant is shown the achieved reward, dependent on precision, by the size of a green bar scaled from 0 (no reward) to 900 pixels (maximum reward). In the case of the presence of a partner, the partner’s score is shown in the same manner via an additional, red-colored bar. Additionally, 500ms after the bars have been shown, the ranking of the participant versus the simulated partner is shown.

2.2 Pre-processing of the Experimental Data

For the data to be fit into the machine learning models, some pre-processing and cleanup had to be performed. This consisted mainly in the removal of unwanted sources, such as eye movement artifacts– this was most prevalent in the channels corresponding to the electrodes closest to the eyes, as ocular movement could very easily get picked up; and electrical noise, and faulty channels, which presented abnormal readings, such as long silent periods, saturation, or strong movement artifact contamination.

From the EEG recordings, we are interested in the interval at the beginning of each trial starting 1000ms prior to the first stimulus onset (see Task Description). At each trial, we will be working with the slice of data starting 1000 milliseconds before and ending 600 milliseconds after the timestamp.

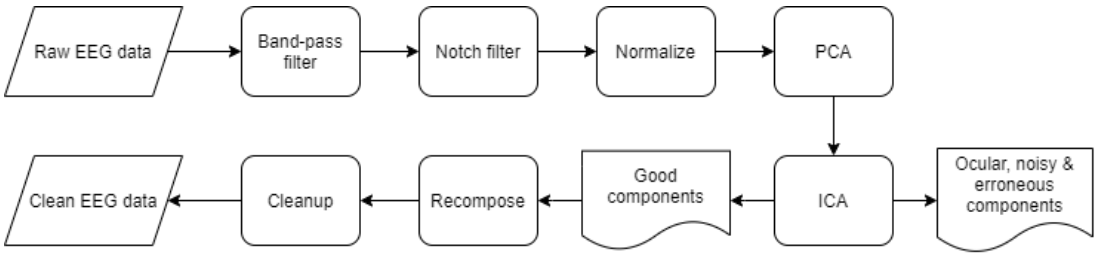

Figure 2. *EEG data pre-processing pipeline.*

Firstly, the data must be pre-processed. We band-pass filtered between 0.5 and 100 Hz and notch filtered at the 50, 100 and 150 Hz, those frequencies that carry electrical noise and its harmonics. The data is then normalized (subtracted the mean and dividing by the

standard deviation or the baseline blocks) and Principal Component Analysis (PCA) is then used to project the data onto a space of eigenvectors expressing the highest variance of the dataset. This allowed us to remove those electrodes that only recorded noise. The next step is to identify those sources that originated in the brain and to remove any other. As a first step, we performed Independent Component Analysis (ICA). In brief, ICA considers the signal recorded at an individual electrode as the sum of several independent source signals. By means of ICA, we de-constructed each channel into several independent components (ICs). We visually checked each component, removing those which we want to leave out of or analysis, such as eye or muscular movements. The remaining data is finally re-composed by performing the inverse process to the ICA. Finally, a second visual inspection of the data is performed in order to identify potentially erroneous channels to be left out altogether.

2.3 Classification

2.3.1 Data Preparation

Since our intent is to compare both sessions and motivational levels, we'll be combining motivational states and trials to form 6 different classes to be compared against each other. Each class corresponds, then, to a motivational level independent of the session it originated from. This results in a matrix with the following dimensions:

$$128 \text{ electrodes} \times 1600 \text{ data points} \times 108 \text{ trials} \times 6 \text{ classes}$$

After reshaping our matrix, we then discard silent channels (those which present a global maximum of 0). This is done as a manner of second proofing in case an erroneous channel was left in during the earlier visual inspection. In case not-a-number (NaN) values are present, these are replaced by the mean value of the channel, as to not sway the models.

2.3.2 1-Nearest Neighbor & Logistic Regression Classifiers

At this point, the data is now suitable to perform our array of analyses on. This part of the study was done using Python, with the *scikit-learn* Python package. Our aim is to generate models which can identify the motivation level and medication status of a participant, given the EEG recording of a trial. We use two different classifiers to fit the models upon which we will perform our analyses: Logistic Regression (MLR) and 1-Nearest Neighbor (1-NN) classification. The MLR is performed using a L2 penalty to avoid overfitting and uses the Limited-Memory BFGS algorithm as solver. In the case of the 1-NN classifier, each sample will be assigned the class of its nearest neighbor, determined by shortest Euclidean distance between features.

2.3.3 Band-pass Filtering & Feature Extraction

The features chosen for classification were electrode power, covariance and correlation, and the classification was performed at three different frequency bands: *alpha* (8 – 12 Hz), *beta* (12.5 – 30 Hz) and *gamma* (30 – 200 Hz). Electrode power will give us an insight into which individual electrodes are responsible for the measured difference in motivation, while covariance and correlation will allow us to see which relationships between electrodes are established and their participation in motivation.

The frequency bands at which we'll measure the data correspond to three of the five widely recognized brain waves emitted by the brain. Each frequency has an associated brain state during which it is more prevalent. Filtering by frequency band, we aim to identify which brain waves the perceived difference in motivation correlates the most with.

Frequency band	Frequency	Brain states
Gamma (γ)	> 35 Hz	Concentration
Beta (β)	12–35 Hz	Anxiety, heightened attention
Alpha (α)	8–12 Hz	Very relaxed, passive attention
Theta (θ)	4–8 Hz	Deeply relaxed, inward focused
Delta (δ)	0.5–4 Hz	Sleep

***Figure 3**. The five basic brain waves and their associated characteristics*[4]

At this point, the process is parallelized into 9 independent sub-processes, each handling a single combination of feature type and frequency band. This is done to drastically reduce computation time, as initial runs of the code could take more than a week to complete for a single participant.

For each combination of feature type and frequency band, the data is first band-pass filtered to contain only the frequencies inside the desired range. A different feature vector is generated depending on the method. Considering the N of channels of our data, in the case of electrode power, this will be a 1-dimensional vector of N size containing the squared mean of each channel. In the case of covariance and correlation, this takes the form of a N×N triangular matrix where, considering *i* and *j* integers between 0 and 128 representing each the index of an electrode, each position *(i, j)* contains the covariance or correlation between electrode *i* and *j*, as calculated below:

$$\text{Cov (x, y)} = \frac{\sum(x_i-\bar{x})(y_i-\bar{y})}{N-1}$$

$$\text{Corr (x, y)} = \frac{\sum(x_i-\bar{x})(y_i-\bar{y})}{\sqrt{\sum(x_i-\bar{x})^2 \cdot \sum(y_i-\bar{y})^2}}$$

***Figure 4**. From top to bottom: covariance (Cov) and correlation (Corr) equations.*

Recursive Feature Elimination is used to select the most informative features. From the 128 features we extracted from electrode power, we'll keep the best 3; in the case of covariance and correlation, since we have 128^2 features, we'll keep the best 90. This will give us an insight on which features have the highest effect

2.3.4 Classification

Labels are assigned to each class. These consist of integers in the range [0, 5], where 0, 1 and 2 represent the three motivational levels (from lowest to highest motivation) during session 1 (off medication), and 3, 4 and 5 represent motivational levels during session 2 (on medication).

A sliding window approach is used to train and test the models. Different training and testing subsets comprising, respectively, the 80% and 20% of the full dataset are generated sequentially 4 times, each with different training and testing sets. The MLR and 1-NN models are fit using the training set, and immediately scored based on the testing set. A testing set with shuffled (and, therefore, erroneous) labels is also used to test the model as control. Each iteration, the results of both testing sets are added to each one's confusion matrix to be analyzed later.

Once all repetitions are complete, the results are plotted and returned to the main process, where they will be further handled.

2.3.5 Analysis

At this point we have already obtained all the data we need for our results, and we have only left to visualize it. Pearson correlation is calculated among the results yielded by the models fit with different training sets across iterations of the sliding window to check stability. The results are plotted by frequency band and measurement.

The most informative features are retrieved and visualized onto a graph of the electrode network: in the case of electrode power, the 10 most informative features, equivalent to the 10 electrodes exhibiting the most change by motivation level, are shown. For covariance and correlation, we show the 20 most informative features – in this case equivalent to electrode connections.

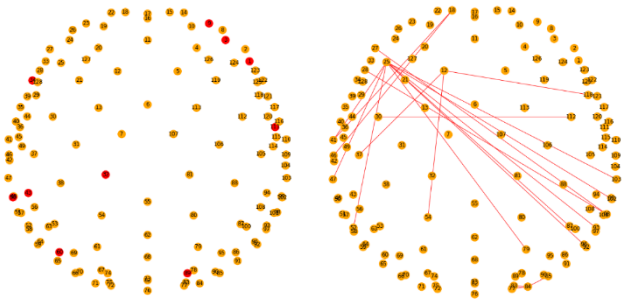

Figure 5. *From left to right:*

- *Map showing the most informative electrodes (highlighted in red).*

- *Graph showing the most informative electrode connections.*

3. Results

Once we have obtained our models' statistics, we can attempt to evaluate the effects of motivation and medication by analysing the accuracy in prediction of each class against the rest. As a reminder, we have a total of 6 classes, one for each combination of motivation level ("low", "medium" & "high") and presence of medication ("off medication" & "on medication"). Prediction accuracy gives us an insight on the identifiability of each of our classes based on our features.

We evaluated our results by **feature type** (electrode power, covariance & correlation) and **frequency band** (alpha, beta & gamma) to determine which features are most indicative of the brain states we observe and at which frequency band they are expressed most significantly.

The figures shown ahead correspond to that of a single participant in the study, but, unless otherwise stated, the observations extracted from them are consistent across the data of all participants. Figures of all participants can be found in the Annex.

3.1 Stability of Results

As mentioned, the stability of the results is calculated using Pearson correlation across the results provided by training and testing the models with different sub-sections of the full dataset using a sliding window approach.

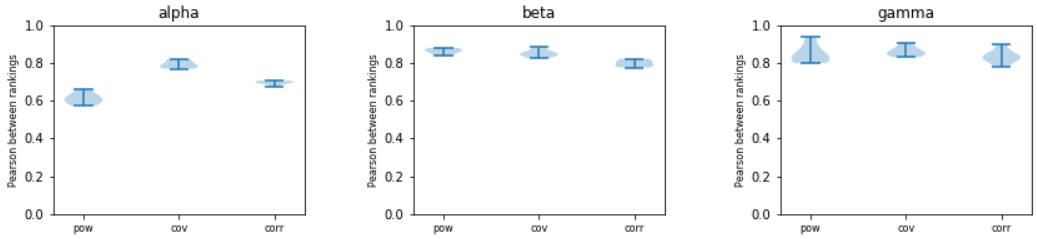

Figure 6. *Comparison of the stability of results by feature type across frequency bands.*

We can observe from the figures that stability increases considerably with frequency band, being alpha the band which yields the lowest stability ranging from 0.6 – 0.8, while beta and gamma show an improved stability in the range 0.8 – 1.

3.2 Identifiability of Motivated Brain States & Effect of Medication

The results obtained from out models were conclusive. From the confusion matrices, we can observe that the error of prediction is very low, reaching even 0 in several cases. These results imply that the identifiability of motivation states based on these features

(electrode power, covariance and correlation) is possible and very accurate, meaning that there is a measurable difference in brain activity inferred by the level of motivation of the person.

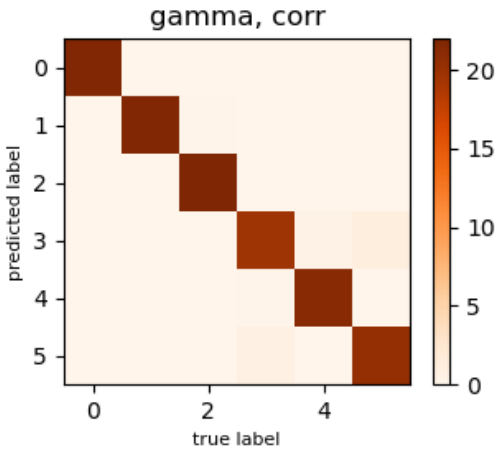

Figure 7. *Confusion matrix across all classes by correlation at gamma frequency band.*

Labels:
0 – Off medication, low motivation
1 – Off medication, medium motivation
2 – Off medication, high motivation
3 – On medication, low motivation
4 – On medication, medium motivation
5 – On medication, high motivation

Classes 3, 4 & 5, representing the states during which the participant had been administered medication, remained each highly distinguishable from the rest, meaning that the brain state of the participant during trials under medication where distinguishable from the rest across all levels of motivation. In order to determine which feature type, frequency band and algorithm can identify our classes most effectively, we'll examine the accuracy obtained by each.

3.2.1 Mean Accuracy by Feature Type & Frequency Band

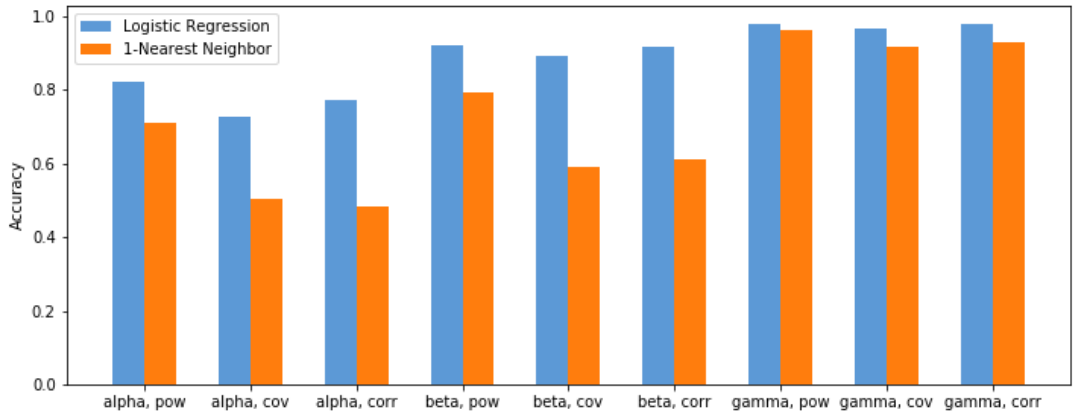

Figure 8. *Mean accuracy of all participants by algorithm across feature types and frequency bands.*

By observing the mean accuracy obtained we can identify several patterns. For one, the Logistic Regression approach consistently obtains significantly better results than 1-Nearest Neighbor algorithm. Additionally, electrode power seems to be the feature type with which the best accuracy is achieved across frequency types, and each frequency band is significantly better than the former. We'll now look in-depth into each category.

3.2.2 Accuracy by Frequency Band

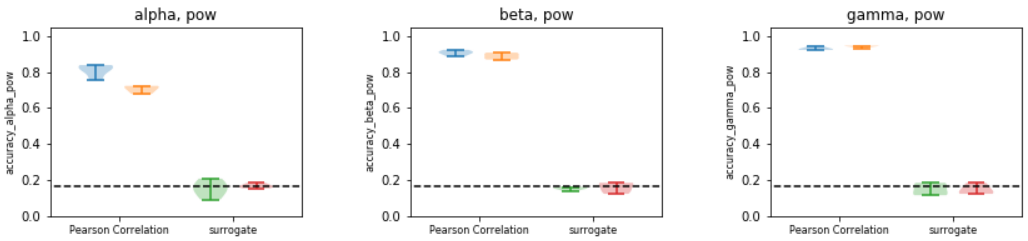

Figure 9. *Accuracy of models by frequency band for a single participant.* *Legend:*
- *Logistic Regression*
- *1-Nearest Neighbor*
- *Logistic Regression (shuffled)*
- *1-Nearest Neighbor (shuffled)*

Comparing across frequency bands reveals a substantial difference. Accuracy becomes progressively higher by increasing frequency: in the case of *alpha*, we obtain an accuracy averaging ~0.8 from the MLR model, and ~0.7 from 1-NN. *Beta* provides an increase in accuracy, bringing the accuracy of both models to an average of ~0.9. The best results are obtained when filtering by the *gamma* frequency band, which slightly increases the average accuracy respective to *beta*, but shows a greatly reduced deviation.

As expected, tests in which labels had been shuffled showed an accuracy around chance level, indicated by the dashed line and corresponding to 1/6.

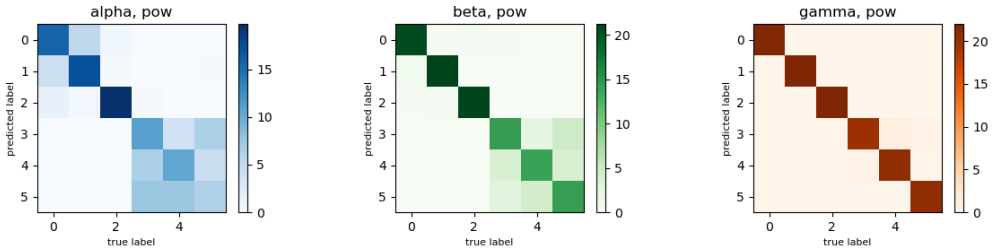

Figure 10. *Confusion matrices by frequency band.*

If we analyze the confusion matrices obtained by frequency band, we can observe how accuracy among motivation states during off-medication trials remain mostly the same, increasing only slightly by frequency band.

It is apparent that off-medication states are more distinguishable from each other at lower frequency bands, at which trials performed under medication show a much worse accuracy in classification.

3.2.3 Accuracy by Feature Type

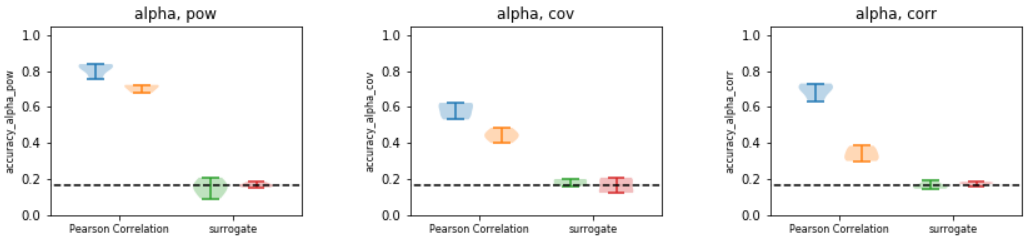

Figure 11. *Accuracy by feature type. From left to right: electrode power, covariance, correlation.*

- *Logistic Regression*
- *1-Nearest Neighbor*
- *Logistic Regression (shuffled)*
- *1-Nearest Neighbor (shuffled)*

When comparing the accuracy obtained using different feature types, we can observe that electrode power stands out as the most accurate. This observation holds true for all frequency bands, but, as we increase frequency, the difference in accuracy is greatly reduced. This is consistent with the observation we made of **Figure 8.**

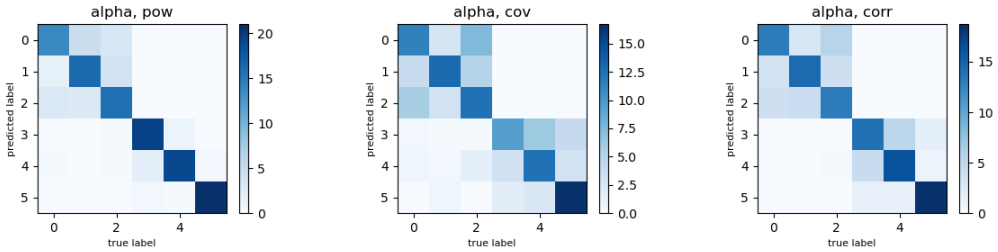

Figure 12. *Confusion matrices by feature type.*

By checking the confusion matrices, we can see how, indeed, electrode power is the feature type that results in the best classification. We can observe how classes corresponding to off-medication and on-medication brain states (classes 0, 1, 2 and 3, 4, 5 respectively) are almost never erroneously classified as the other, hinting at a strong distinction between brain states depending on the presence of medication.

3.3 Brain Activation by Region & Most Informative Features

As previously mentioned, through Recursive Feature Elimination we were able to rank our features by informativeness and keep the ones most useful to this prediction. This way, we can identify which brain areas are determinant of the brain states we observe, as well as which connections are established.

3.3.1 Activation by Brain Area

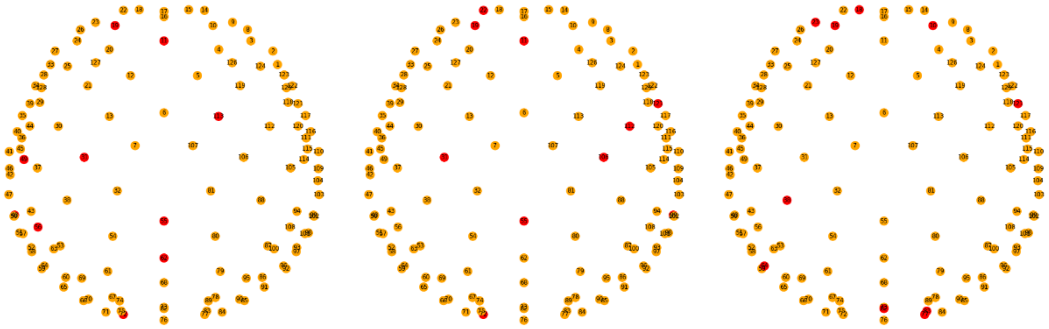

Figure 13. *Most informative electrodes for a participant (highlighted in red). From left to right: alpha, beta, gamma.*

By analyzing the most informative features in the case of electrode power, we can identify which areas of the brain are most indicative of the brain states defined by our classes. Unfortunately, observing the results obtained by the RFE across participants, we cannot identify any recurring patterns.

3.3.2 Established Connections

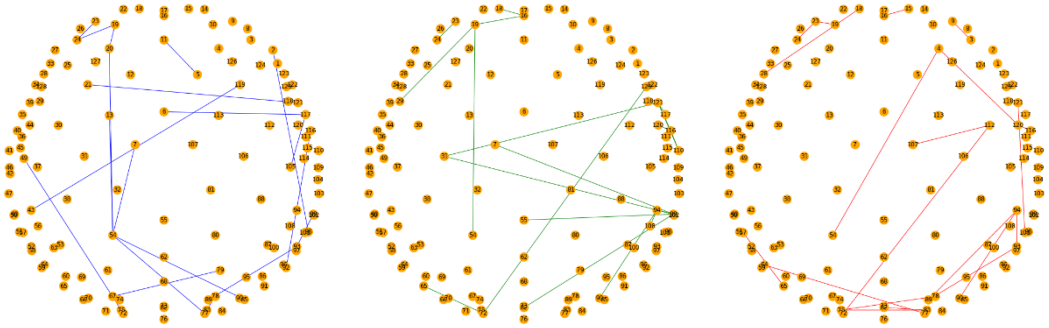

Figure 14. *Most informative covariance relationships for a participant. From left to right: alpha, beta, gamma.*

We can see from the most informative covariance & correlation relationships as obtained by RFE that the observations made in the last section hold true – no recurring patterns can be established.

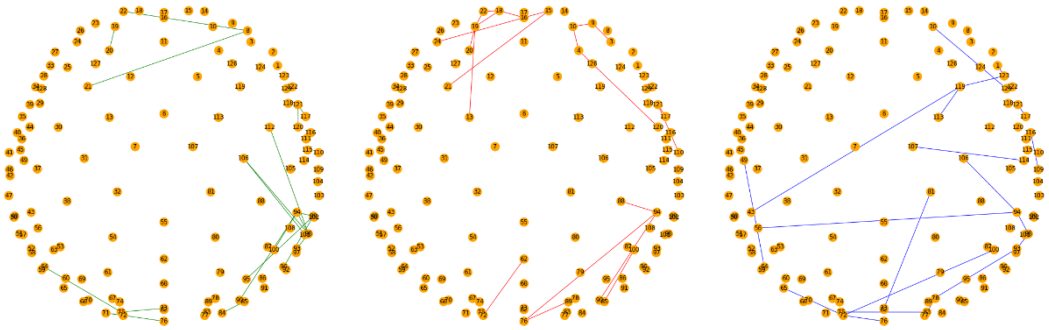

Figure 15. *Most informative correlation relationships for a participant. From left to right: alpha, beta, gamma.*

4. Discussion

With this study, our goal was to identify a relationship between states of motivation and physiological brain states which we could identify based on a series of characteristics obtained from EEG recordings of cerebral activity. Additionally, we wanted to test if the effect of dopaminergic medication could be comparable to that of heightened motivation levels on Parkinson's disease patients. To this end, an experiment was conducted in which the participants were instructed to perform a movement accompanied by a simulated virtual partner which they would be scored against in order to induce a sense of competition and increase motivation. Throughout the experiment, a 128 electrode EEG device recorded brain activity.

The data was band-pass filtered into the *alpha, beta* and *gamma* frequency bands and fitted into two independent machine learning algorithms: Logistic Regression (MLR) and 1-Nearest Neighbor (1-NN). Three different sets of features were used: electrode power, covariance between electrodes, and correlation between electrodes. Recursive Feature Elimination (RFE) was applied to each feature set in order to select the most informative features of each set. We predicted that this, in addition to optimizing the models generated by the algorithms, would give us some insight into which brain regions and connections between them are affected by motivation and presence of dopaminergic medication.

Both machine learning algorithms generated models which could identify motivational states, both on-medication and off-medication, with high accuracy. In particular, the best approach was found to be MLR, on the *gamma* frequency band, using electrode power for features. This combination achieved near perfect classification of our testing sets across all participants. Electrode power consistently proved better accuracy than its counterparts, but this difference was reduced on higher frequency bands, being this difference almost unnoticeable on the gamma band. These results reveal that motivation state can indeed be identified by brain activity, and the brain states resulting of different levels of motivation can be characterized.

We can observe how on-medication brain states consistently show more error in prediction among them at lower frequency bands. Increasing frequency band bring about a drastic increase in accuracy.

Furthermore, we cannot establish a relationship between presence of medication and a state of motivation, as on-medication and off-medication states were distinguished from each other with almost perfect accuracy. Even in the lesser accurate models (e.g. those

fit with covariance on data filtered on the *alpha* band) error in classification between classes of different sessions was extremely rare.

Analysis of most informative features yielded no conclusive results. The most informative electrodes and electrode connections were different across participants, and no patterns were apparent. It is possible that this is product of classifying off-medication and on-medication states together as a single set of classes, as we found that they hold no significant relationship. Defining two separate sets of classes for each session independently of the other and running RFE off those might reveal a pattern of most informative features for motivation states in each case.

5. References & Bibliography

1. "Neuroscience" *Merriam-Webster Medical Dictionary* http://c.merriam-webster.com/medlineplus/neuroscience
2. Kriegeskorte, Nikolaus; Douglas, Pamela K. (September 2018). "Cognitive computational neuroscience" *Nature Neuroscience* https://www.ncbi.nlm.nih.gov/pmc/articles/PMC6706072/
3. Deco G, Jirsa V, McIntosh A. Emerging concepts for the dynamical organization of resting-state activity in the brain. Nat Rev Neurosci. 2011; 12:43–56. doi: https://www.nature.com/articles/nrn2961 PMID: 21170073
4. Priyanka A. Abhang Bharti W. Gawali Suresh C. Mehrotra "Technological Basics of EEG Recording and Operation of Apparatus" https://www.sciencedirect.com/science/article/pii/B9780128044902000026

- scikit-learn – Machine Learning in Python: https://scikit-learn.org/stable/
- matplotlib: https://matplotlib.org/
- NumPy: https://numpy.org/

6. Appendix

6.1 Model Stability Across Feature Types by Frequency Band

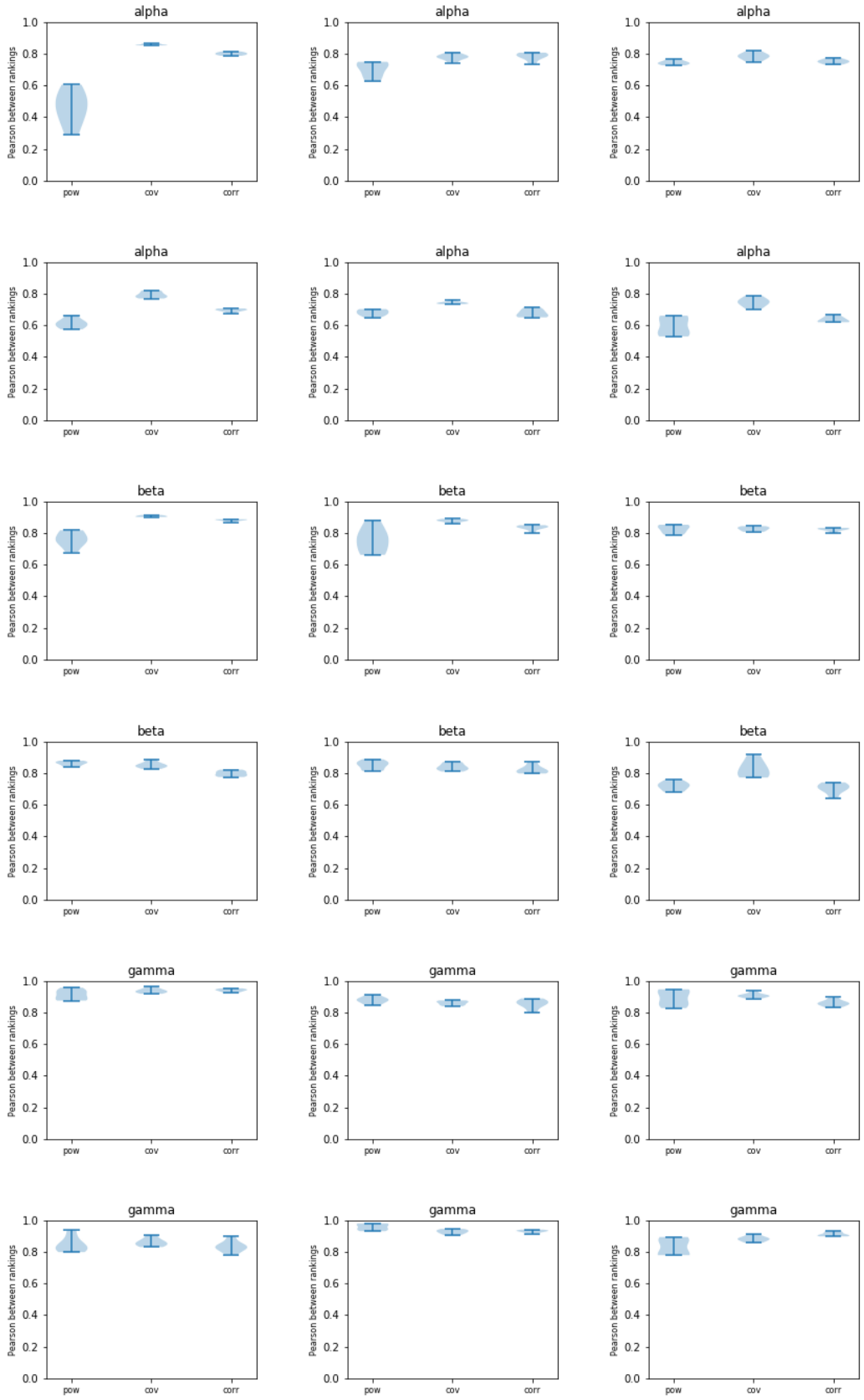

6.2 Model Accuracy by Feature Type and Frequency Band

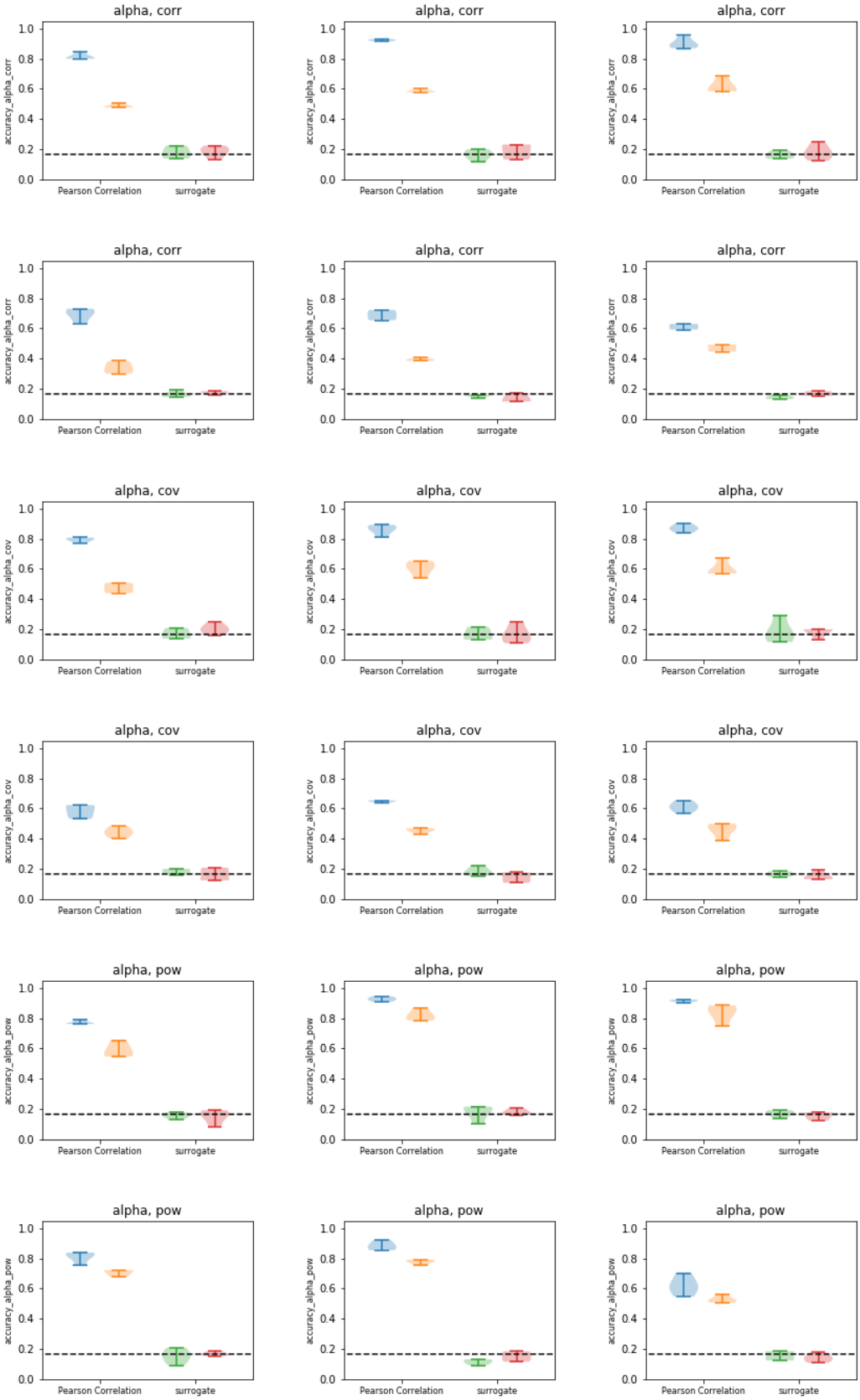

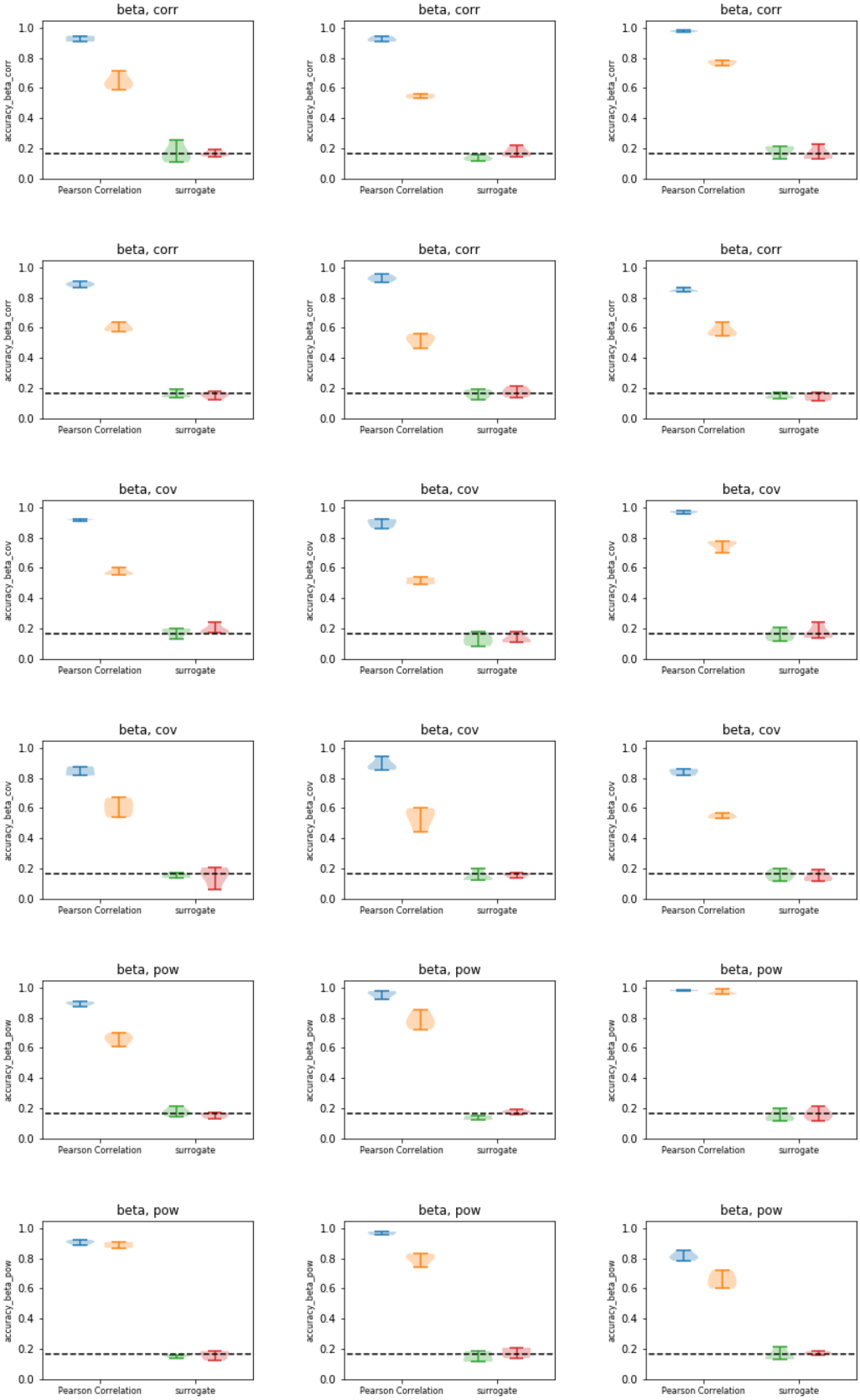
beta, corr
beta, corr
beta, corr
beta, corr
beta, corr
beta, corr
beta, cov
beta, cov
beta, cov
beta, cov
beta, cov
beta, cov
beta, pow
beta, pow
beta, pow
beta, pow
beta, pow
beta, pow
accuracy_beta_corr
accuracy_beta_cov
accuracy_beta_pow
0.0
0.2
0.4
0.6
0.8
1.0
Pearson Correlation
surrogate

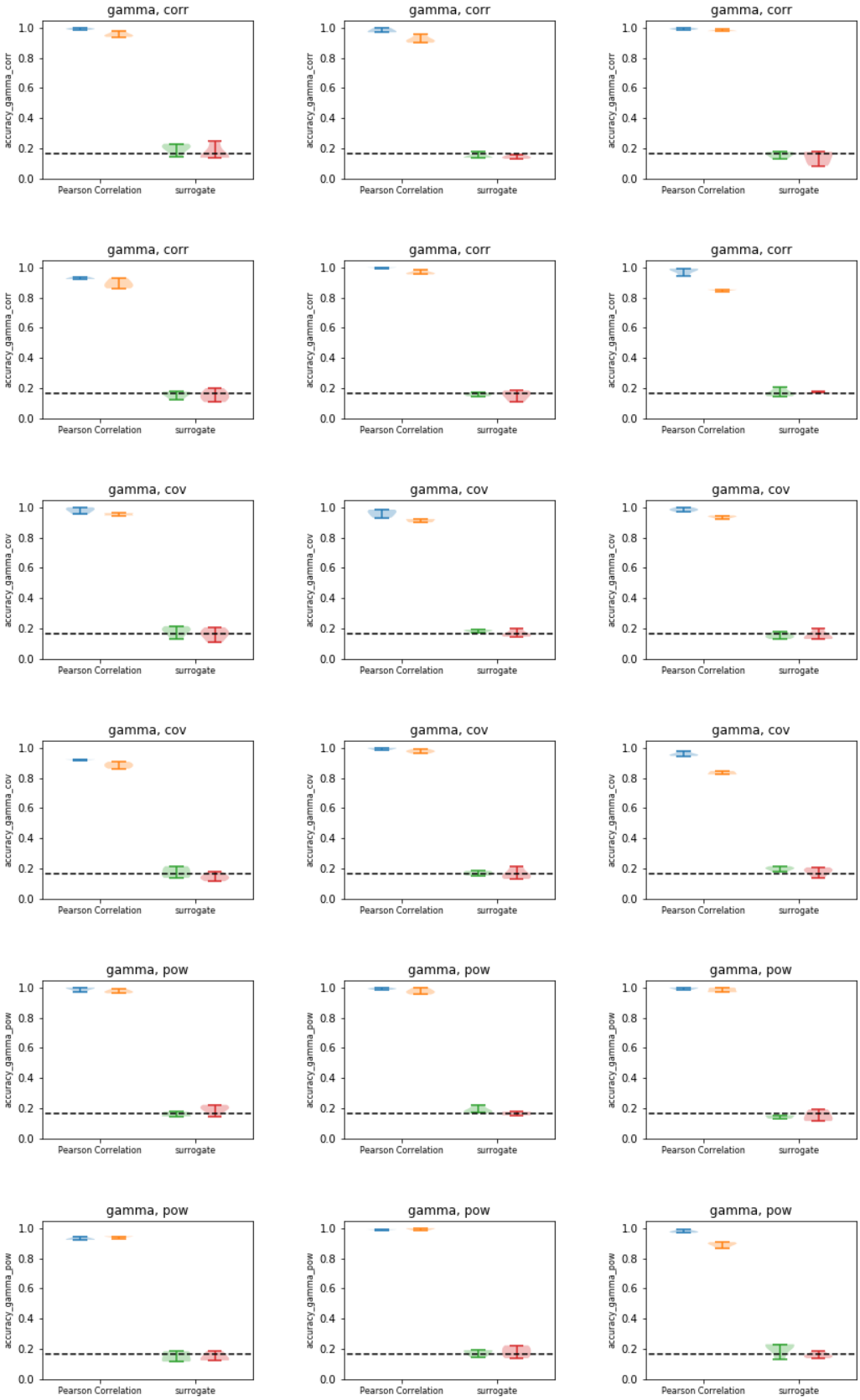
gamma, corr
gamma, corr
gamma, corr
gamma, corr
gamma, corr
gamma, corr
gamma, cov
gamma, cov
gamma, cov
gamma, cov
gamma, cov
gamma, cov
gamma, pow
gamma, pow
gamma, pow
gamma, pow
gamma, pow
gamma, pow
accuracy_gamma_corr
accuracy_gamma_cov
accuracy_gamma_pow
0.0
0.2
0.4
0.6
0.8
1.0
Pearson Correlation
surrogate

6.3 Confusion Matrices by Feature Type and Frequency Band

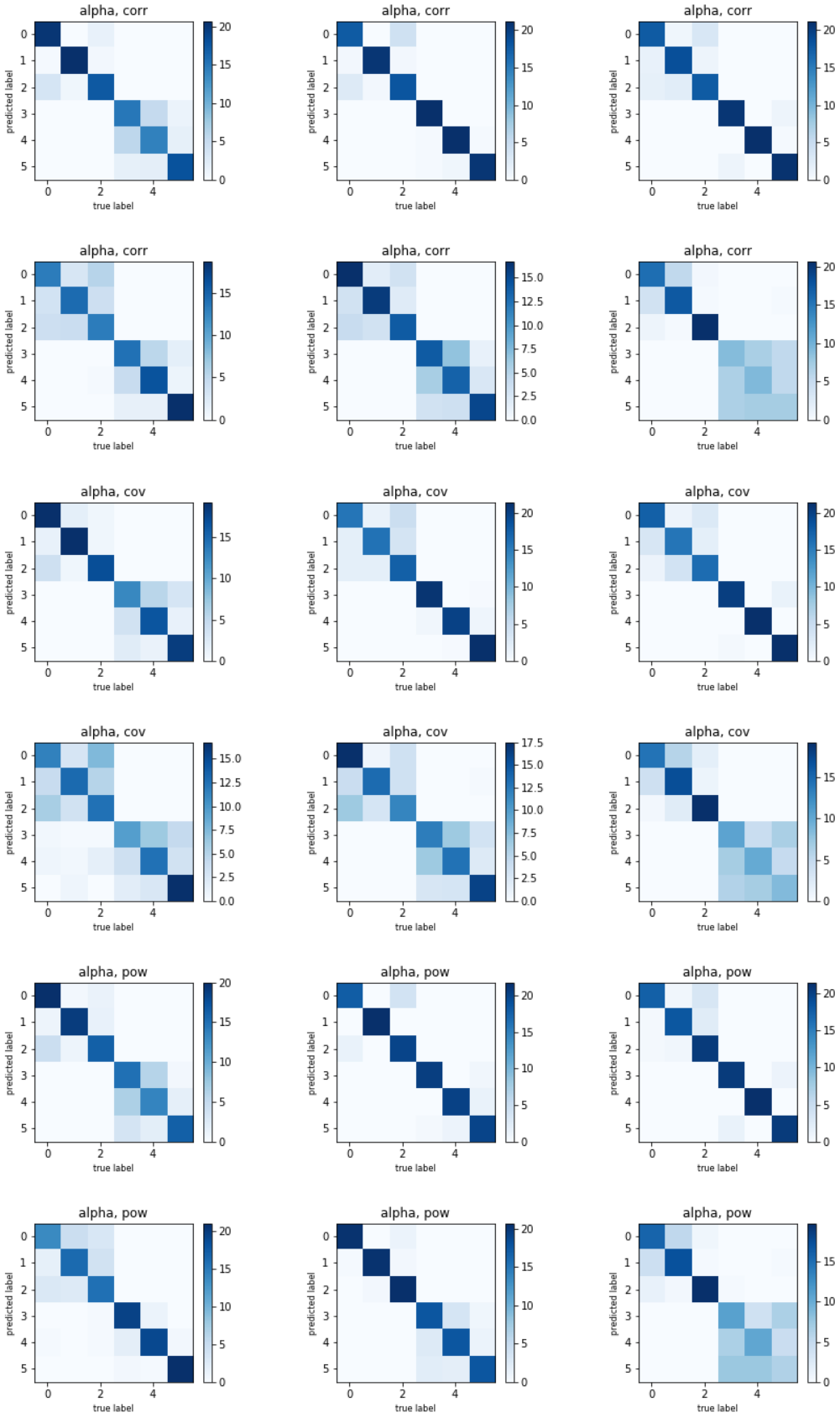

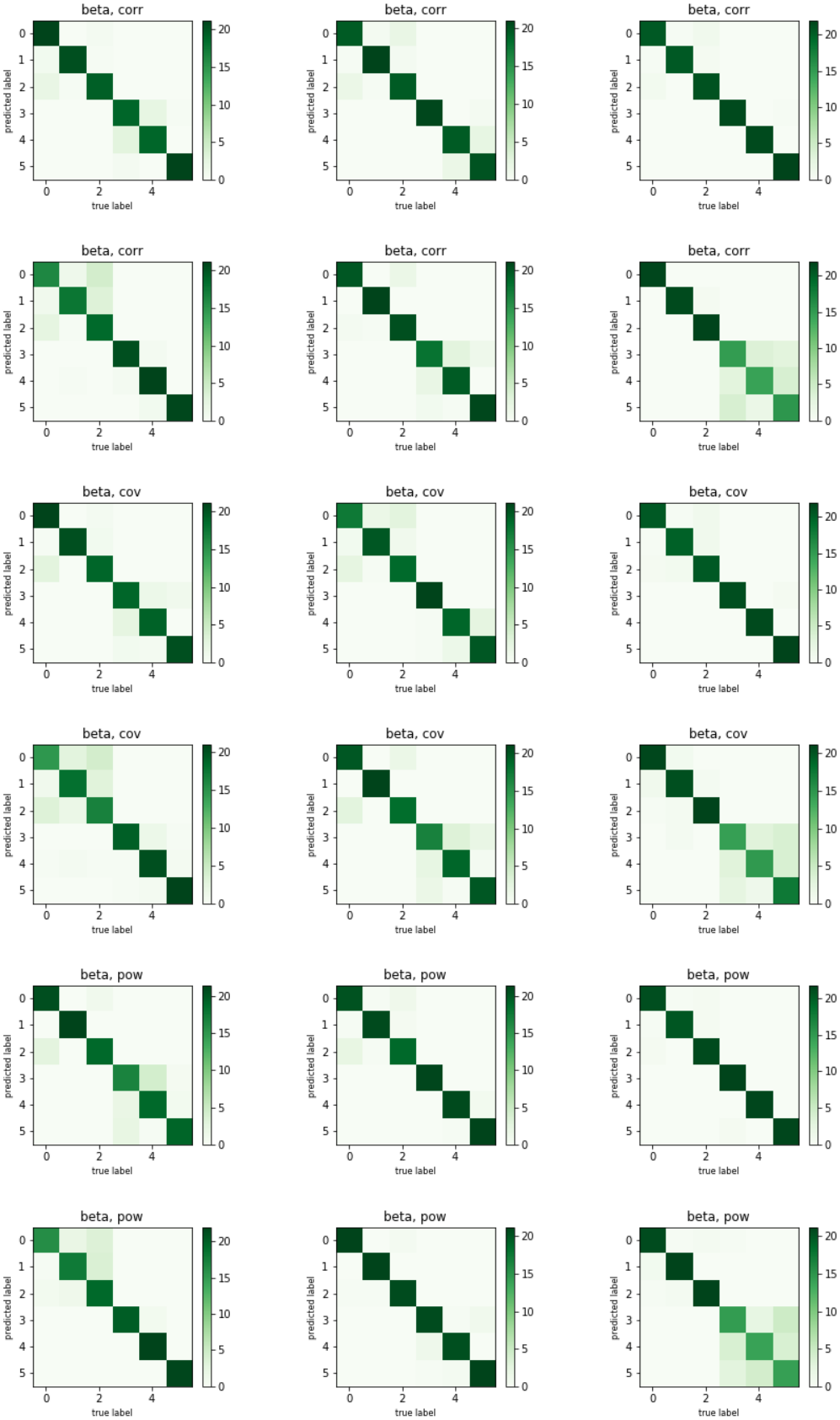
beta, corr
beta, corr
beta, corr
beta, corr
beta, corr
beta, corr
beta, cov
beta, cov
beta, cov
beta, cov
beta, cov
beta, cov
beta, pow
beta, pow
beta, pow
beta, pow
beta, pow
beta, pow
predicted label
true label

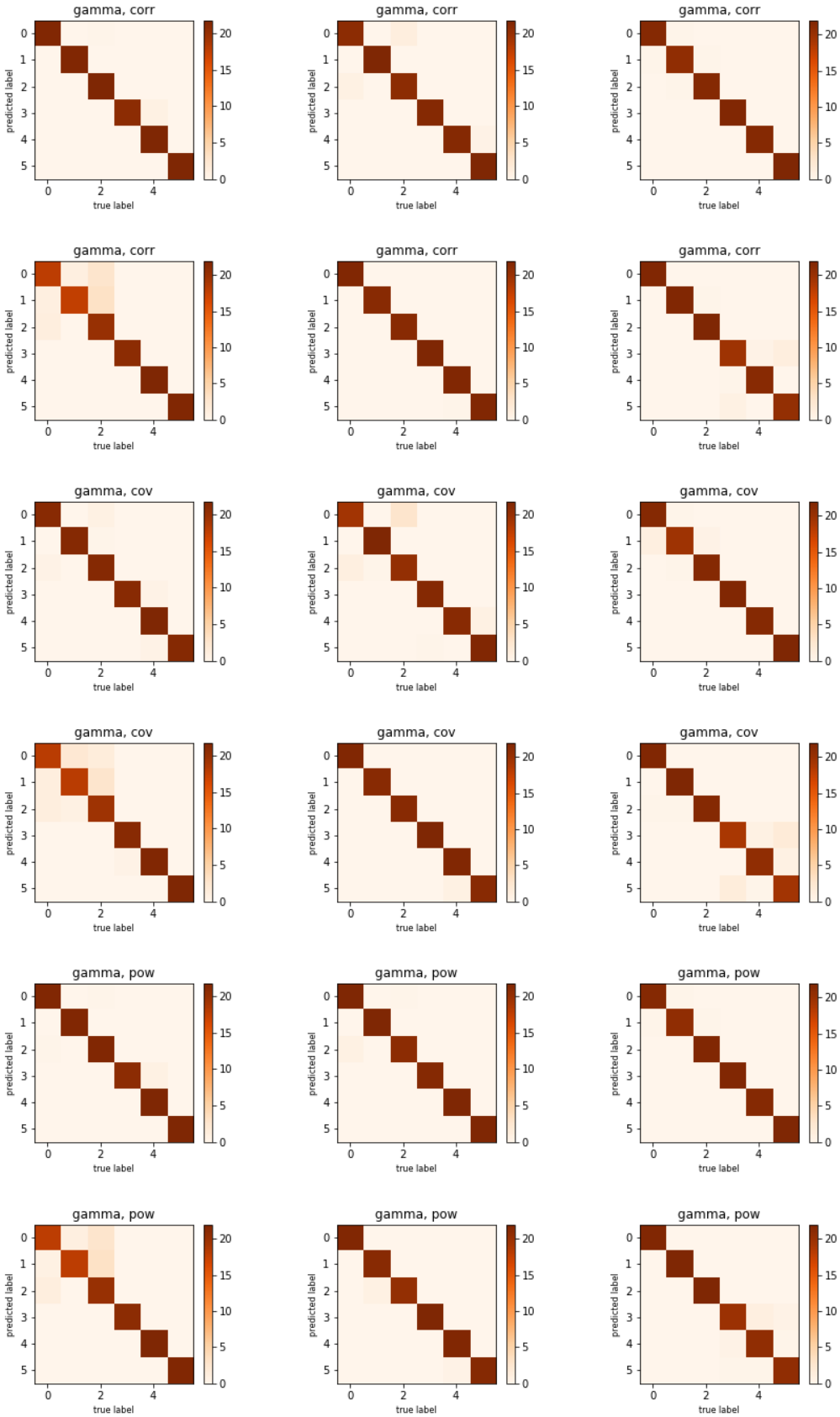
gamma, corr
gamma, corr
gamma, corr
gamma, corr
gamma, corr
gamma, corr
gamma, cov
gamma, cov
gamma, cov
gamma, cov
gamma, cov
gamma, cov
gamma, pow
gamma, pow
gamma, pow
gamma, pow
gamma, pow
gamma, pow
predicted label
true label

6.4 Mean Accuracy Across Feature Type and Frequency Band by Participant

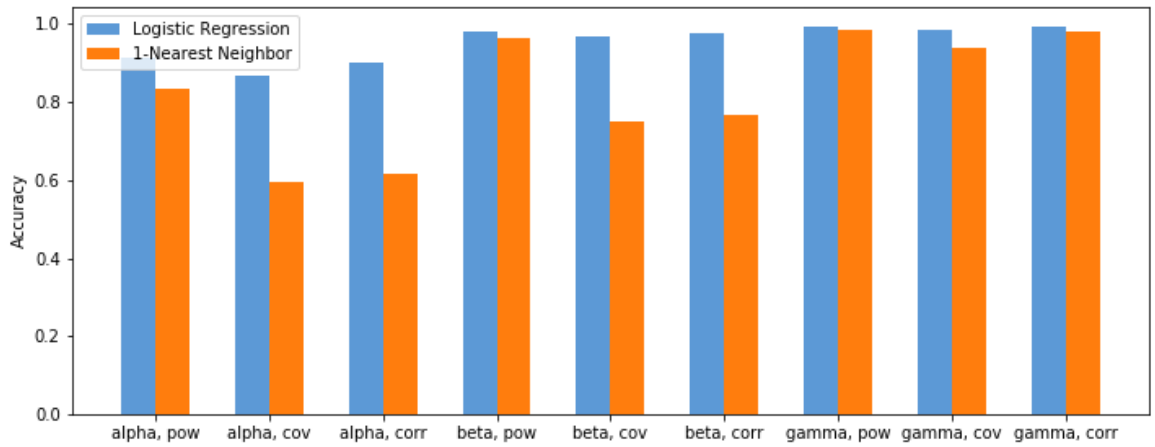

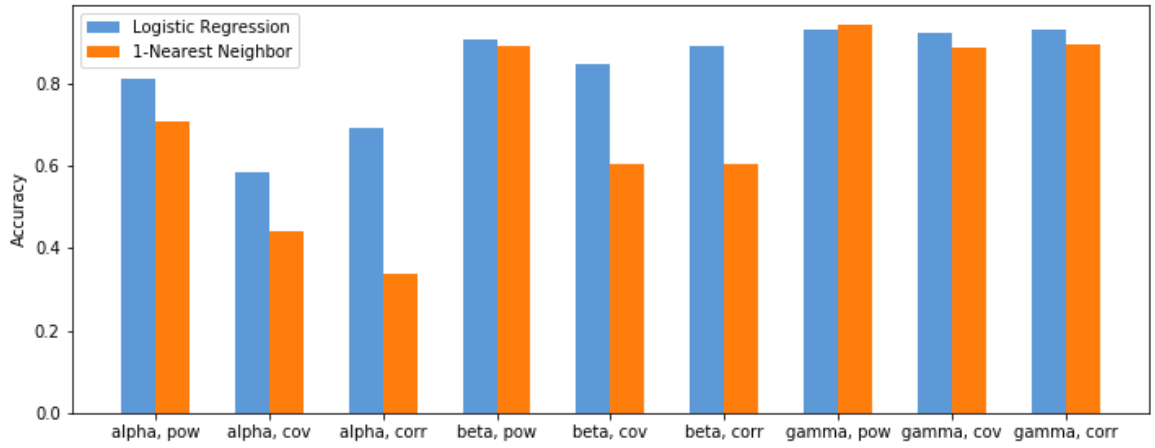

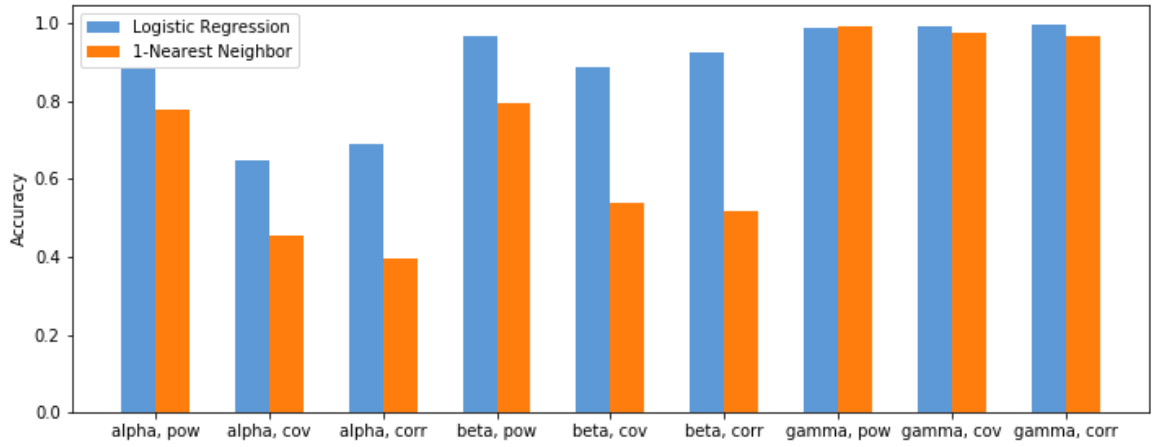

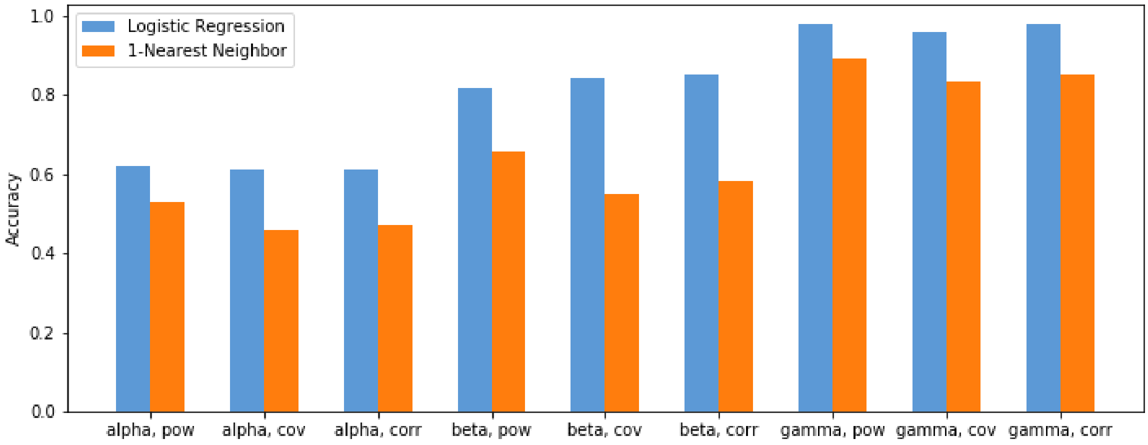
Logistic Regression
1-Nearest Neighbor
Accuracy
1.0
0.8
0.6
0.4
0.2
0.0
alpha, pow
alpha, cov
alpha, corr
beta, pow
beta, cov
beta, corr
gamma, pow
gamma, cov
gamma, corr

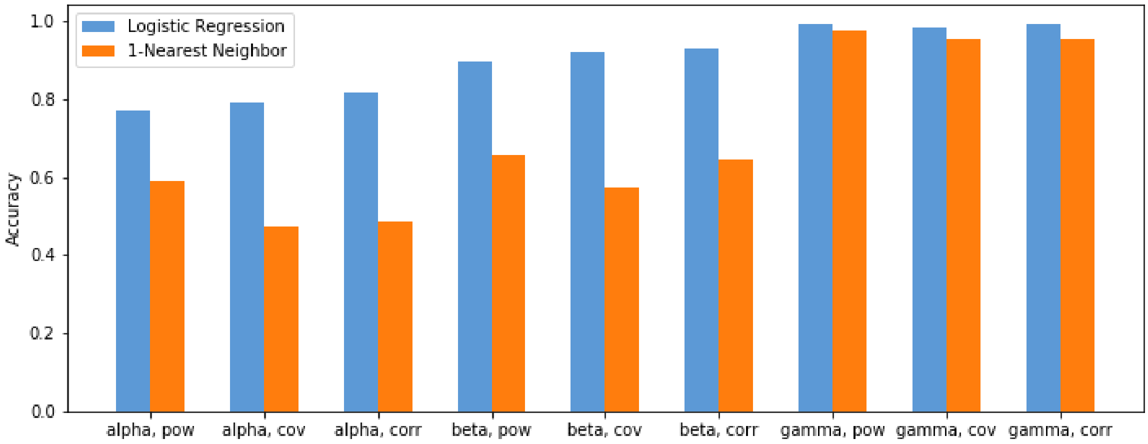
Logistic Regression
1-Nearest Neighbor
Accuracy
1.0
0.8
0.6
0.4
0.2
0.0
alpha, pow
alpha, cov
alpha, corr
beta, pow
beta, cov
beta, corr
gamma, pow
gamma, cov
gamma, corr

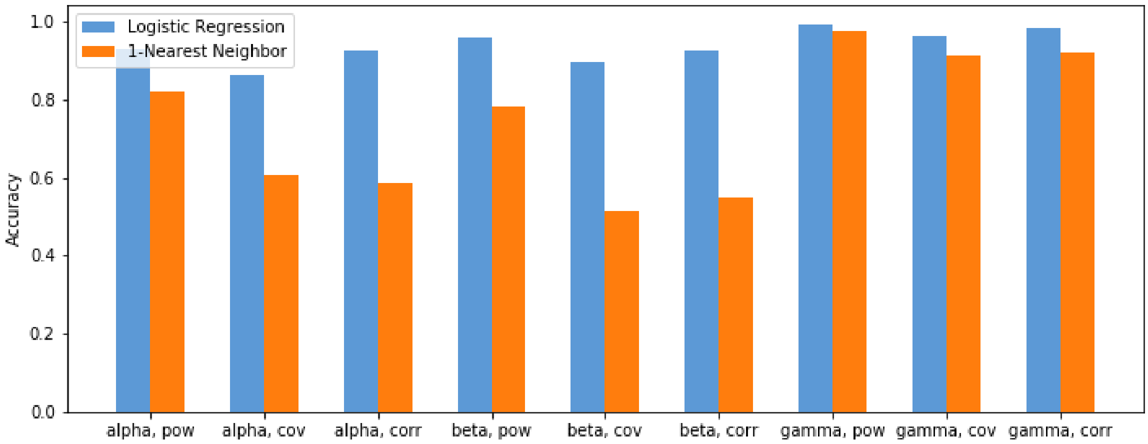
Logistic Regression
1-Nearest Neighbor
Accuracy
1.0
0.8
0.6
0.4
0.2
0.0
alpha, pow
alpha, cov
alpha, corr
beta, pow
beta, cov
beta, corr
gamma, pow
gamma, cov
gamma, corr

6.5 Most Informative Correlation Relationships by Frequency Band

- *Alpha*
- *Beta*
- *Gamma*

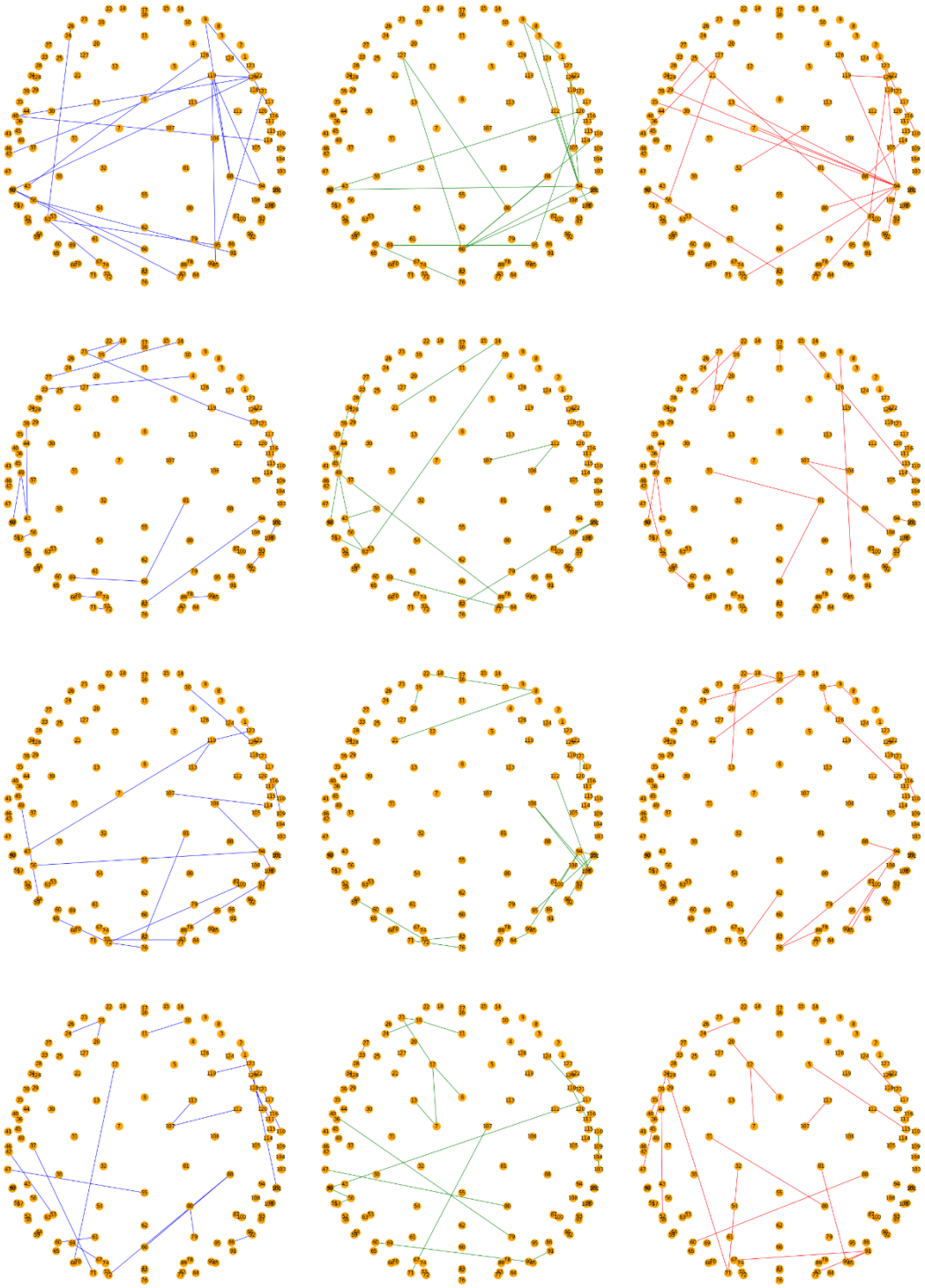

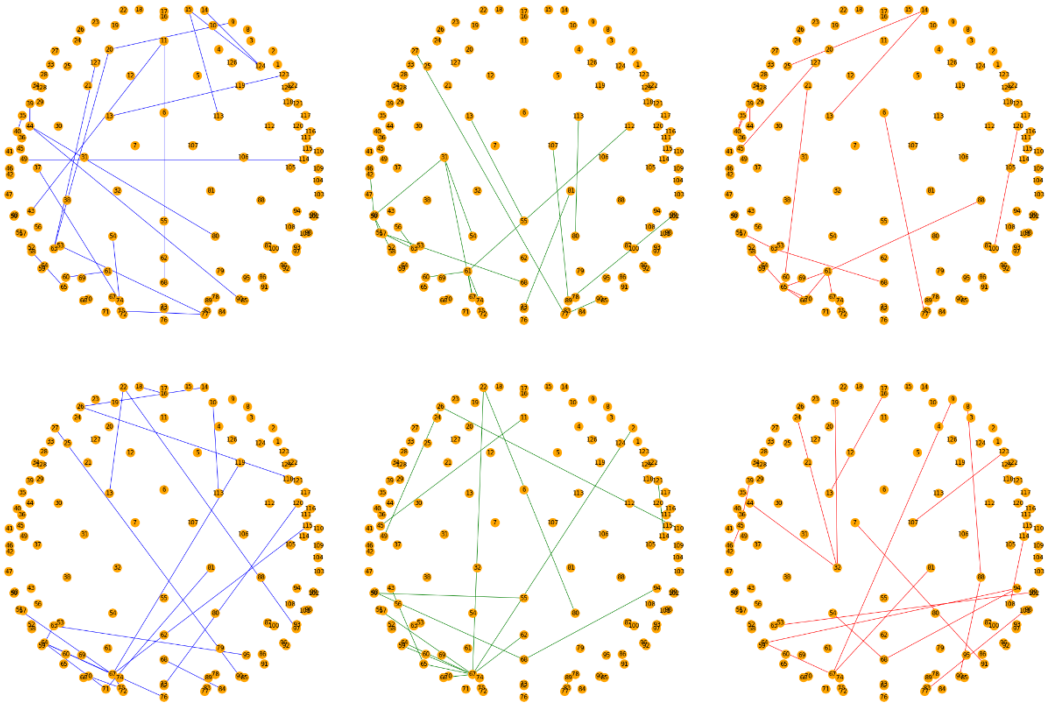

6.6 Most Informative Covariance Relationships by Frequency Band

- *Alpha*
- *Beta*
- *Gamma*

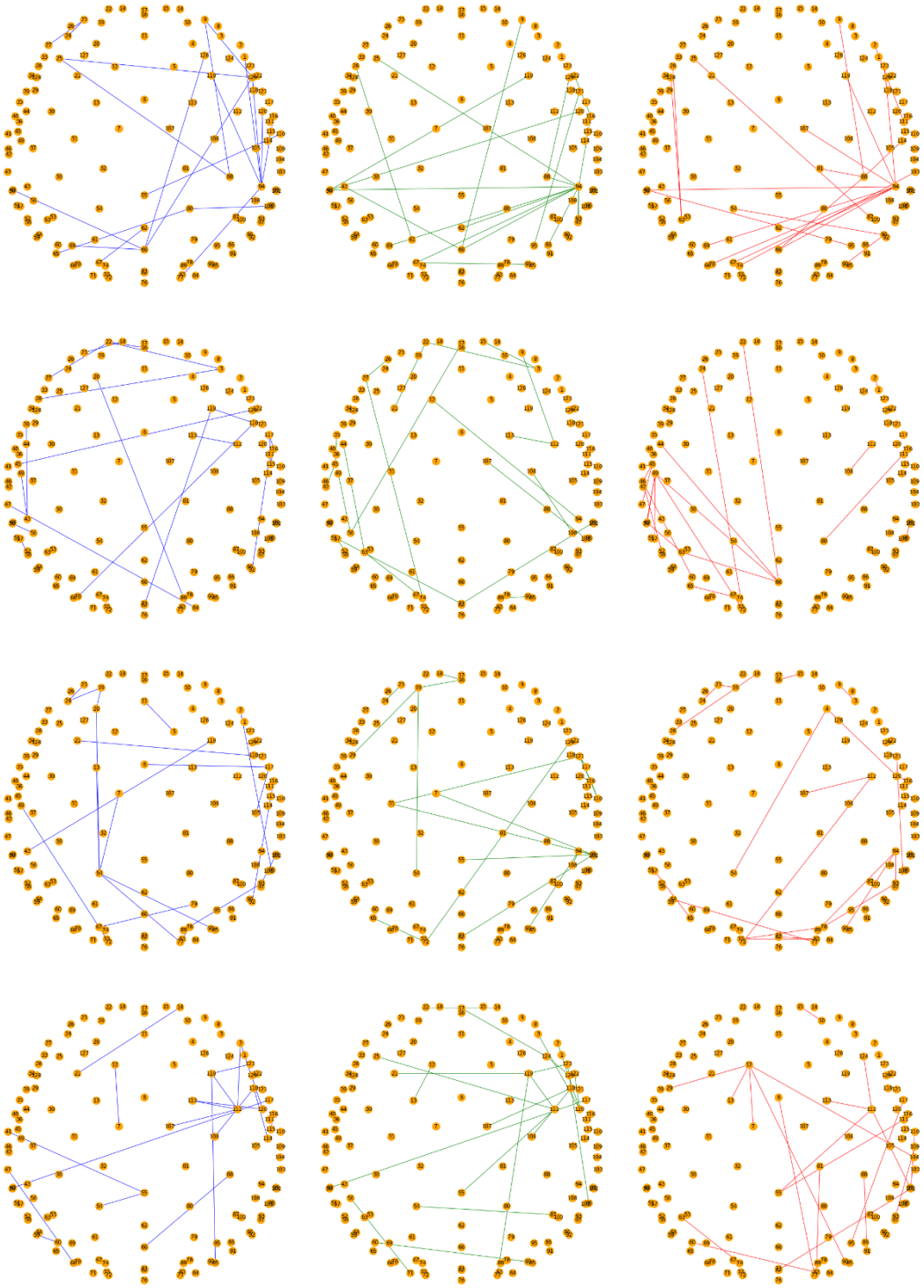

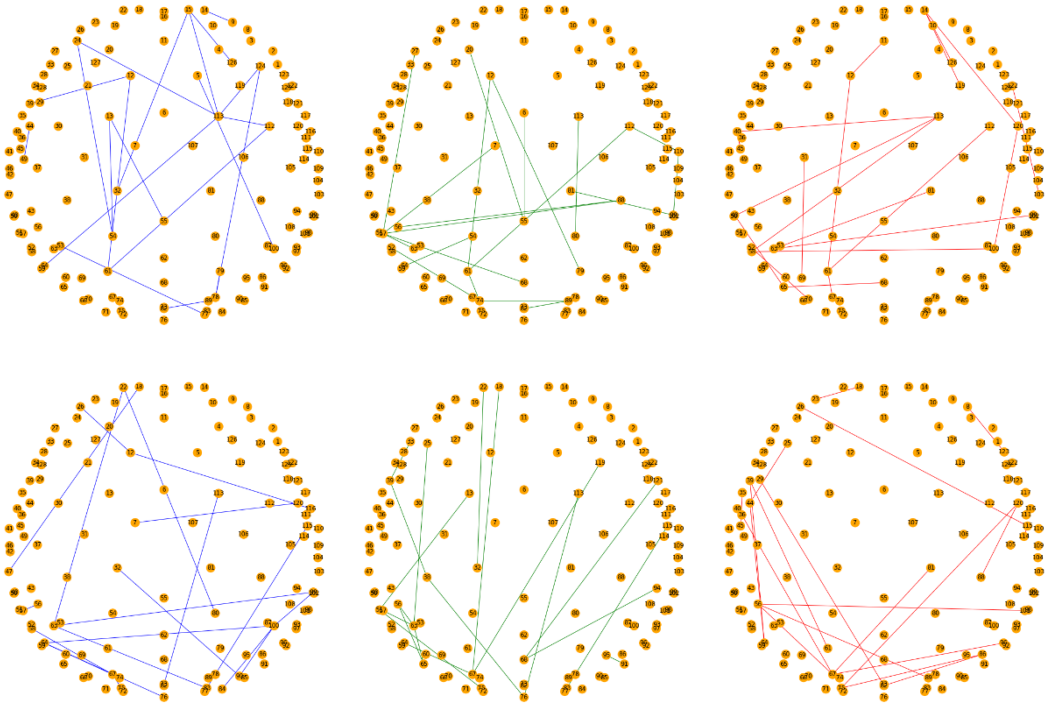

6.7 Most Informative Electrode Power by Frequency Band

- *Alpha*
- *Beta*
- *Gamma*